



# Bioderived Hygromorphic Twisted Actuator for Untethered Sustainable Systems

Reece Whatmore<sup>1</sup>(✉), Emelia Keely<sup>1</sup>, Zoe Lee<sup>2</sup>, Adriane Minori<sup>3</sup>, and Lining Yao<sup>3</sup>

<sup>1</sup> Department of Materials Science and Engineering, Carnegie Mellon University, Pittsburgh, PA 15218, USA

{rwhatmor, ekeely}@andrew.cmu.edu

<sup>2</sup> Industrial Design Department, Rhode Island School of Design, Providence, RI 02903, USA  
zlee@risd.edu

<sup>3</sup> Human-Computer Interaction Institute, School of Computer Science, Carnegie Mellon University, Pittsburgh, PA 15218, USA

aminori@andrew.cmu.edu, liningy@cs.cmu.edu

**Abstract.** Environmentally friendly and hygromorphic actuators have gained increasing attention for energy harvesting, field robotics, seeding and biodegradable active structures and sensors. While recent works have used hygromorphic seeds as sources of bio-inspiration, it is challenging to engineer synthetic hygromorphic actuators with comparable stiffness, energy density, and reaction speed, and the processing of synthetic materials or need for external power sources inevitably increases fossil fuel consumption and waste production. In this paper, we harness an alternative bioderived design approach, utilizing the natural twisted body of the seed, *Hesperostipa Sparteae*, itself as a sustainable and biodegradable hygromorphic twisting actuator that converts atmospheric water concentration into mechanical energy. Our self-powered twisted actuator is capable of providing twisting actuation with a load over 11,000 times its body mass. We further demonstrate the potential of modular biohybrid design to create untethered self-locking and crawling systems, powered solely by environmental stimuli. The ability to create biodegradable self-actuating systems with modular bioderived design presents opportunities to create biocompatible systems, improving sustainability in the field of soft robotics and beyond.

**Keywords:** bioderived and biohybrid design · morphing materials · active smart materials · hygromorphic motion · twisting actuator · sustainable robotics

## 1 Introduction

Nature provides endless sources of inspiration for designers and engineers. With climate change posing a threat to our society and planet, it is essential that we create sustainable systems that generate less harm to the natural world. One way to increase the compatibility between mechanical design and natural ecosystems is to create systems that are

---

**Supplementary Information** The online version contains supplementary material available at [https://doi.org/10.1007/978-3-031-38857-6\\_17](https://doi.org/10.1007/978-3-031-38857-6_17).

built of natural materials, tailored to harness renewable energy, and fully biodegrade. We can build further upon the principles of bioinspiration by using a bioderived design that harnesses organic materials in their natural form to create a fully biocompatible system.

One common source of self-powered actuation in nature is hygromorph. Moisture triggers a mechanical response in hygromorphic materials, causing materials such as wood and many seeds to morph with humidity changes in the atmosphere. Previous works have harnessed the hygromorphic ability of wood to enable untethered and self-sensing actuation as an inherently moisture-responsive material in architecture [1], design [2], robotics [3], and 3D printing [4, 5]. Other hygroscopically induced actuators have been made with biobased materials such as paper[6], thin wood laminates [7, 8], large wooden bilayers [9, 10], and 4D printing biobased composites [11, 12]. Additionally, other humidity-driven materials such as agarose [13] and polyethylene oxide films [14] have been used to create humidity-powered robotic locomotion.

Many natural seeds are hygromorphic, which have been presented as sources of bioinspiration for past works. In natural environments, oscillations in humidity and temperature conditions occur throughout the day and night transition cycle which stimulate the seeds' shape changes [15]. The self-powered motion and unique forms have inspired an array of bioinspired seed-actuators that have been used for motions such as microflyer flight [16], self-drilling [17, 18] lifting [19], and coiling [20]. While these past works took the natural seeds as bio-inspirations, we propose an alternative bioderived approach, harnessing an organic seed itself as a sustainable natural actuator.

In this work, we investigate the porcupine grass seed, *Hesperostipa Spartea*, as an untethered self-sensing and powered actuator for potential robotic applications. The *Hesperostipa Spartea* is a species of perennial grass that is native to the Great Plains of North America [21]. It has a tightly twisted awn that generates torque to power its humidity-driven self-burial behavior [22]. We study their behavior to harness their twisted awn as natural and off-the-shelf actuators and to potentially enable other custom-made bioinspired actuators. We hypothesize that since the twisted bodies of the porcupine seed are tight and dense with respect to other coiled seeds (e.g., *Erodium*), we can harness a more advantageous time-response and actuation performance for soft and biohybrid robots. Furthermore, by leveraging the seed itself without post processing (e.g., chemical washing [17]), we maintain the integrity of the seed's strength and performance. To validate this hypothesis, we investigate the morphology and biomechanics of the seed, including its actuation strain, speed, and strength-to-weight ratio, and demonstrate its usability towards sustainable and biohybrid robotic applications (e.g., self-locking, crawling).

## 1.1 Background: *Hesperostipa Spartea*

The porcupine grass seed, *Hesperostipa Spartea*, is a hygro-responsive seed that harnesses humidity fluctuation for a self-burial motion [21]. The complete seed diaspore can be described in three distinct sections: the pointed tip (s1), extended awn (s2 and s3), and bent end (s4) (Fig. 1A, 1B). The sharply pointed tip consists of a hairy callus containing the seed embryo. The awn sprouts from the seed's tip in a twisted section that begins tightly twisted (s2) and transitions into looser twists (s3) as it approaches the

bend. The end of the seed has a bent, untwisted portion (s4), sometimes with the double-bent structure. The twisted section provides the mechanical twisting of the seed and will be classified as the body of the seed throughout this paper. While the internal structure of the specific *Hesperostipa Sparteae* seed has not been explored in detail, the internal structure holds similar to the *Stipa Epilosa* seed [23]. The structure of the seed can be described as a combination of two planes of lighter (p1) and darker (p2) shade, with the lightest shaded edge plane (e1) connecting these two, respectively (Fig. 1C, 1D). The internal structure of the two intertwined twisted bilayers allows for the reversibility of the twisting and untwisting of the segment as stimulated by humidity fluctuations (Fig. 1E). The basic kinetic shape change of the seed is a reversible humidity-driven untwisting and retwisting motion to provide mechanical energy for the seed's self-burial behavior. When the seed is exposed to humidity in the air or submerged in water, it transforms from its initial pre-twisted state to an untwisted, elongated state, by rotating in a clockwise direction, when viewed from above, with the seed tip downwards. The internal structure of the seed holds shape-memory, resulting in a repeatable motion. When the seed is fully untwisted and is exposed to a dry (low humidity) environment, or removed from high humidity conditions, it begins to retwist in a clockwise direction. When isolating the body of this seed, it can be mechanically viewed as a self-powered twisted actuator as a function of the humidity diffusion rate. The twisted body holds potential to be harvested for many applications beyond its natural burial behavior.

## 2 Biological Investigation

Porcupine grass seeds, *Hesperostipa Sparteae*, were purchased online from Everwilde Farms. The seed's diameter was measured using a Carbon Fiber Composites Digital Caliper with a resolution of 0.1 mm. The seed mass was measured with a U.S. Solid Precision Balance with a resolution of 10–5 g. Seed characteristics including seed length and seed twist angles were conducted using ImageJ software with a pixel resolution of 2532x1170. The seeds were placed in water and a humidity chamber to stimulate their untwisting motion, and the water and air temperatures were measured with a smart sensor infrared thermometer.

### 2.1 Analysis of *Hesperostipa Sparteae* Geometry as a Hygroscopic Actuator

An analysis on the seed characteristics was conducted to understand the geometric parameters of the biological material. Due to the bioderived nature of our design, our ability to optimally construct a robotic system depends on our ability to both quantify and control the natural deviation within the seeds. We focused on quantifying the twisted body of the seed to understand its geometry and its resulting rotational shape changes. From this analysis, a method of harvesting with maximum consistency was developed to create a geometrically quantifiable twisted actuator.

The twist angle of the seed is defined as the angle from the seed's edge to its closest dark plane (Fig. 1F). When in its dry twisted state, the twist angle was quantified with a sample size of 13 natural *Hesperostipa Sparteae* seeds (e.g.,  $n = 13$  for the following angle and twist number measurements). The complete seed has  $14.15 \pm 1.6$  twists in its total

length (complete extended awn), and the tightly twisting portion (s2) has an average of  $10.84 \pm 1.1$  twists, resulting in an average of  $3.90 \pm 0.32$  mm per seed twist. The average angle of the twists in the seed is  $24.71 \pm 1.95^\circ$ . The twists in the region extruding from pointed tip (s2 in Fig. 1A) have the tightest and most consistent twist with an average angle of  $22.60 \pm 2.29^\circ$ . At the opposing end of the awn (s3 in Fig. 1A), towards the bend, the twists become wider and hold more variation, with an average angle of  $26.47 \pm 2.82^\circ$ . As a result of this variation in twisting angles, when harvesting the seeds as a twisting actuator, the seed length is limited to the section containing consistent tight twists (s2), on average a length of  $42.11 \pm 3.26$  mm.

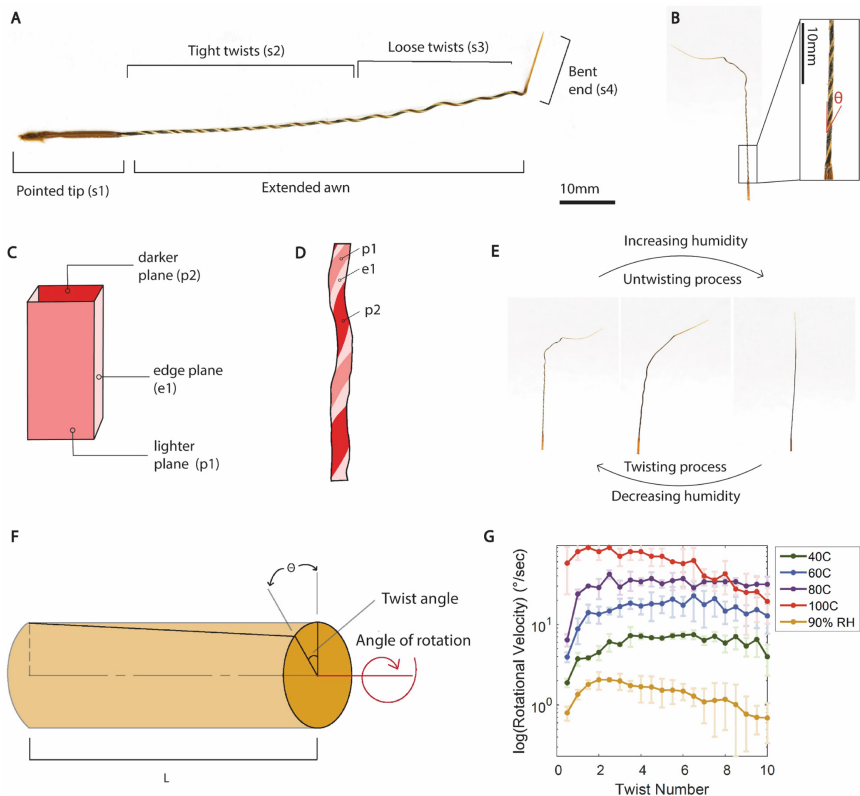


**Fig. 1.** Porcupine grass seed characteristics. (A) Anatomy of porcupine grass seed. (B) Porcupine grass seed with magnified image of tight twists near the pointed tip. (C) Schematic of seed planes. (D) Schematic of seed fully twisted, with the dark, edge, and light planes depicting the twists of the seed. (E) Twisting and untwisting process of seed at various times given an increase or decrease in humidity. (F) Cross-sectional schematic of seed demonstrating the angle of rotation of twists, and the twist angle of the seed. (G) Number of twists in a seed relative to the log scale of rotational velocity. Rotational velocity is the degree of untwisting per second given various temperatures of water and relative humidity levels. Data are means with standard deviations shown with error bars given  $n = 3$  samples.

We additionally analyzed the rotational speed of the seed to further quantify actuation time. The speed of the seed's rotational actuation is a function of humidity level and temperature (Fig. 1G). Among the conditions tested, fastest actuation speeds occur under highest temperature and complete water submergence (i.e. in  $\sim 100^\circ\text{C}$  hot water) from the twisted to untwisted state. The rotational speed from the dehydrated to hydrated state was tested in a humidity chamber with 90% relative humidity, and in water at 40, 60, 80 and  $100^\circ\text{C}$  temperatures. The maximum rotational speed in hot water submergence is much faster than when the seed is actuated under atmospheric humidity conditions (Fig. 1G). When transitioning from the twisted state to an untwisted state, the maximum speed in  $100^\circ\text{C}$  hot water submergence was  $90^\circ/\text{sec}$ , while in a controlled 90% relative humidity environment under room temperature at  $\sim 21^\circ\text{C}$ , the maximum speed was  $2.05^\circ/\text{sec}$  (Fig. 1G). The samples tested did not experience any visible damage under high temperatures. However, further morphological and mechanical tests are needed to understand how high temperature conditions may impact the reversibility of the system. To minimize actuation time, warm temperature and high relative humidity conditions should be used to stimulate the seed's natural motion. However, the shape changes of the twisting behavior remains identical, independent of temperature or humidity level. This allows for seed's actuation to be stimulated in a variety of environmental conditions, expanding the potential of the seed to a further breadth of applications.

## 2.2 Humidity Driven Strain Measurement

**Preparation and Tracking of Seeds in Humidity Chamber.** A humidity chamber was used to control environmental relative humidity levels for analyzing the seed's twisting morphology. To calculate the strain under controlled varying humidity conditions, the seed's motion was tracked while in the humidity chamber. Clay stands were molded to support the seeds, and each bend of the seed was tagged with a small piece of electrical tape for optimal tracking purposes (Fig. 2A). The seeds were placed in a controlled chamber held at a constant temperature of  $22^\circ\text{C}$ , with monitored humidity level, reaching a maximum of 90% relative humidity (Fig. 2A). Humidity and temperature were monitored using the DHT-22 humidity sensor and Arduino UNO. The tag on each seed was tracked using Tracker, a video analysis and modeling software program, to record the change in the vertical extension of the seed with time. The percent strain was calculated with  $\frac{l-l_0}{l_0}$  and plotted against the relative humidity within the chamber (Fig. 2B).

**Strain Results.** The seed's unique twisted structure and hygromorphic design allows it to withstand stresses when in humid atmospheres. To compare the relative humidity and strain of the seed, and thus, the deformation it can undergo, an experimental stress analysis was conducted. After a period of initial negative strain, the strain of the body increases with humidity, and reaches its maximum percent strain as the humidity in the chamber is standardized to 90% relative humidity (Fig. 2B). An increase in humidity causes elongation of the seed relative to its initial length: a humidity level of 90% results in a maximum strain of 25% of the seed's body. Before the 90% humidity level is reached, the seed undergoes a negative strain as a result of the end of the seed near the loosely twisted region bending while untwisting from a dehydrated to hydrated state. After upwards of 40 min, 90% humidity is reached, at which point the tighter twists

near the pointed tip begin untwisting and elongating, creating an overall positive strain (Fig. 2B).

A strain analysis of the seed with the bend removed, portions s1-s3 of the seed, demonstrated a similar initial period of negative strain before elongation. A minimum percent strain of  $-7.34\%$  ( $\pm 3.95$ ,  $n = 3$ ) occurred due to the bending of the loosely twisted portion of the seed (s3) while transitioning from a dehydrated to hydrated state (Fig. 2Cii). The seed continues to untwist throughout the hydration process, reaching extension and resulting in a final maximum percent strain of  $9.18\%$  ( $\pm 2.9$ ,  $n = 3$ ) (Fig. 2Civ). From these observations, we can hypothesize that the negative strain observed in the initial humidity strain test (Fig. 2B) is due to this bending of s3 compounded with further bending due to the weight of the tracking tag. The seed's tightly twisted portion (s2) shows no bending motion and therefore shows no period of negative strain. The tightly coiled region has a maximum percent strain of  $15.25\%$  ( $\pm 1.36$ ,  $n = 3$ ) (Fig. 2D).

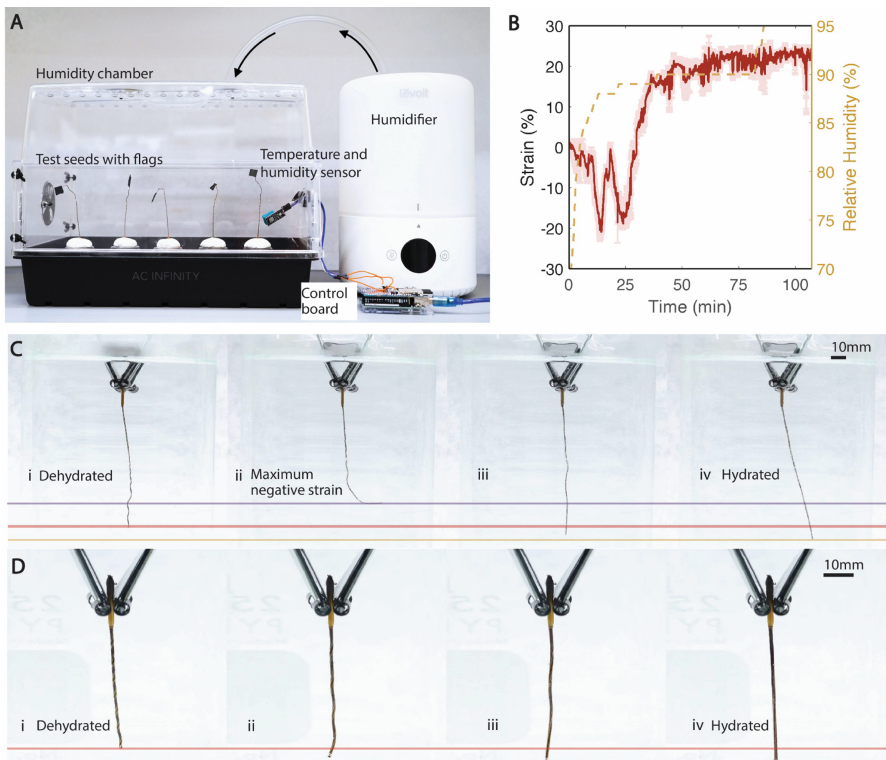


**Fig. 2.** (A) Experimental humidity chamber setup with tagged seeds that untwist from their initial dehydrated state to their final, untwisted hydrated state. (B) Percent strain of seed as relative humidity increases to 90%. Data are means with standard deviations shown in the shaded regions given  $n = 3$  samples. (C) Time lapse photos of seeds untwisting in hot water, depicting the negative strain in a seed when loose and tight twists are present. (D) Time lapse photos of seeds untwisting in hot water, depicting the positive strain when the seed is cut so only tight twists are present in the seed.

### 2.3 Load Lifting Test

As a further investigation into the mechanical properties of the seed, a weight lifting analysis was conducted. The total lift distance and rotational speed as the seed transitioned from an initial untwisted state to a completely retwisted state was analyzed under varying loads (completed in a heated ~ 30–50 °C environment). To control variation in the organic structure, the bend (s4) was trimmed to 10 mm when in a dry state. Each seed was then fully untwisted in hot water, the pointed tip (s1) was removed, and all seeds were cut to a length of 60 mm. This process of controlled harvesting creates an optimized bioderived actuator. Four completely untwisted seeds were hung vertically with clips with four differing loads attached (0 g, 50 g, 100 g, 200 g) (Fig. 3A). Seeds were placed in a heated chamber and the distance each seed lifted its corresponding mass was measured.

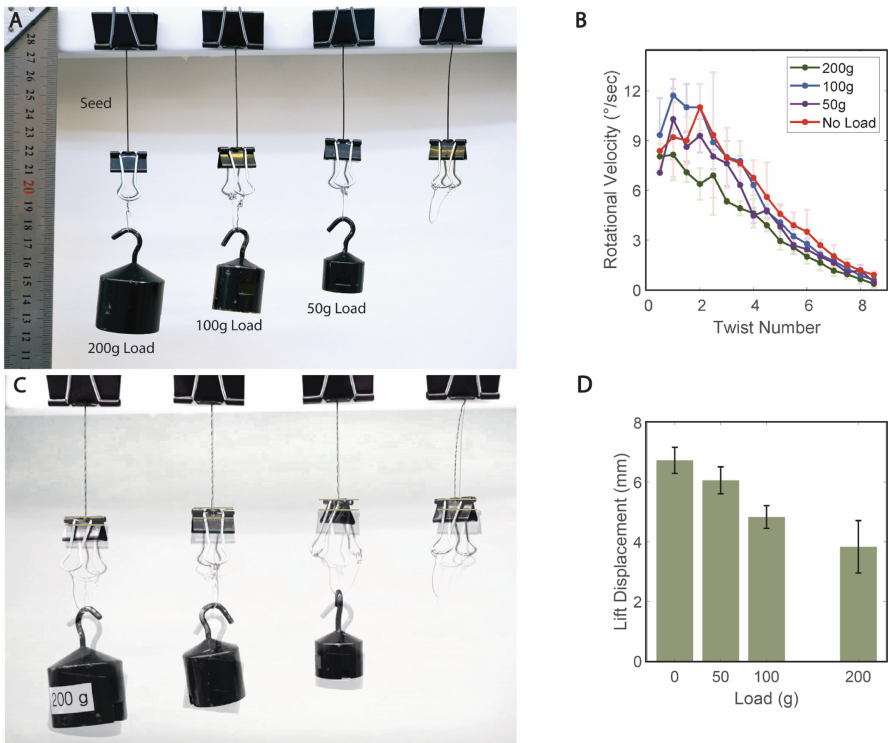


**Fig. 3.** (A) Experimental load lifting test setup with fully untwisted seeds bearing loads of 0, 50, 100 and 200 g. (B) The rotational velocity of the seed relative to its number of twists for the various loads lifted. Data are means and the error bars represent standard deviations given  $n = 3$  samples. (C) Time lapse of seeds lifting their loads as they transition from hydrated to dehydrated states. (D) Lift displacement, calculated as the difference in height of the load as the seed twists from its initial hydrated state to its final twisted dehydrated state. Data are means and the error bars represent standard deviations given  $n = 3$  samples.

The rotational velocity ( $^{\circ}/\text{sec}$ ) of the seed varied under load with the fastest rotation occurring under no load and slowest under the largest (e.g., 200 g load) (Fig. 3B). A 200 g load is over 11,700 times larger than its body mass (average seed mass is  $0.017 \pm 0.002$  g,  $n = 10$ ), demonstrating the ability for the seed to continue its twisting shape change and remain a functional twisting actuator under extremely large relative loads. The seeds were further demonstrated to translate their twisting motion to a load lifting actuation (Fig. 3C). There is an inverse relationship in the mass of the load and the distance of lift (Fig. 3D). The seed's ability to lift a load over 11,700 times its mass further demonstrates the remarkably powerful morphomechanics of the seed. Both the twisted actuation and lifting movements are powered solely by the seed's kinematic material properties under environmental stimuli. The lifting motion represents the ability to leverage the seed to create an organic self-powered and untethered system. Moreover, this lifting justifies the seed as a bioderived twisted muscle capable of providing both twisted actuation and lifting with extremely high relative loads.

### 3 Demonstrations of Harvesting *Hesperostipa Spartea* Seed as Hygromorphic Twisted Actuator

#### 3.1 Interlocking Systems

**Preparation and Execution of Seeds for Interlocking Test.** To minimize variation, the length of each fully untwisted seed in the procedure was 80 mm in length. The dry seeds were placed in hot water until they fully untwisted, and were then cut to 80 mm, leaving the bend intact. Two seeds were placed on a platform with their bends facing towards each other, and their point ends supported by a 500 g weight. The seeds were positioned so they overlapped by 65mm, and a heater was positioned in front of them to accelerate the locking process (Fig. 4A). After the locking process, one end of the seed system was attached to a clip and hung vertically (Fig. 4B). A clip was attached to the other end of the system, and masses were hung incrementally, every 30 s. The maximum mass supported was that which caused the seeds to untwist.

**Interlocking Demonstration.** Through harnessing the natural kinetic motion of the seeds, we produced an intertwined two-seed interlocking system (Fig. 4C, 4D). The natural morphology of the seeds allows for untethered locking with response to environmental humidity change. During a wet to dry humidity cycle the system transitions from an unlocked to locked state, while a dry to wet state reversibly unlocks the system. The bioderived design of this system harnesses both the bent portion of the seed awn (s4) and the twisted body of the awn (s2 and s3). The natural bend in the end of the seeds provides optimal grasping to create a tight double twist (Fig. 4D). We controlled the geometric parameters of the length of the bend, length of the twisted body, and distance overlapped of the seed to create an efficient and consistent locking mechanism (Fig. 4A). With a 10 mm bend length (dry twisted state), 80 mm body (wet untwisted state), and 65 mm overlap (wet untwisted state), an average of  $3.8 (\pm 0.75, n = 6)$  intertwined twists were created (Fig. 4C, 4D). The resulting entwined two-seed system creates an environmentally stimulated reversible self-locking system. The lock was able to hold an average load of  $113 \text{ g} \pm 20.7, n = 6$  samples, over 3,400 times the mass of the two-seed system



(Fig. 4B). Beyond locking as a mechanical feature, this design demonstrates the modular potential of the biderived twisted actuators. Through harnessing this interlocked design to create multi-actuator systems, future application opportunities may arise for moisture triggered docking mechanisms, self-entangled active structures, etc.

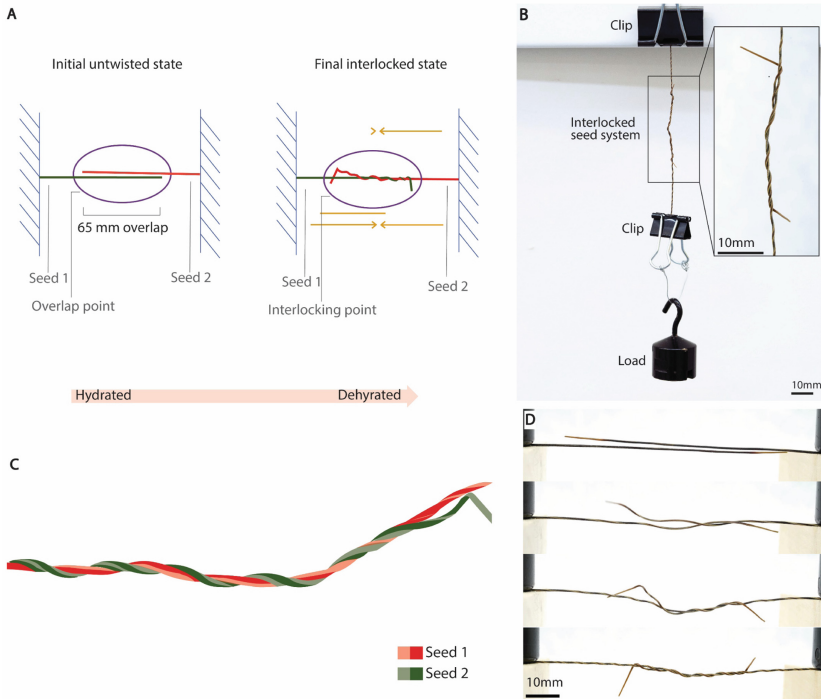


**Fig. 4.** Locking seed system schematics. (A) Schematic of seed interlocking experimental setup. Seeds overlap by 65 mm and interlock with increasing humidity. (B) Experimental setup for interlocked seed system load test. (C) Schematic of interlocking between two seeds. (D) Time lapse of two seeds locking together as humidity and temperature increase.

### 3.2 Biohybrid Crawling Design and Development

**Design and Implementation.** We harvested the tightly twisted body (s2) of the seed to create a biohybrid crawling robot. By controlling the geometry of the seed's body, a humidity-responsive twisted actuator that converts atmospheric water concentration into mechanical energy is achieved. The biohybrid structural design enables periodic crawling locomotion to occur. Through the addition of fixed circular “wheels”, the crawling biohybrid design transfers the twisting motion of the seed's body into a rolling locomotion (Fig. 5A). The motion is driven solely by environmental stimuli and does not require any additional energy input, creating an untethered system.

The biohybrid design consists of a combination of laser cut wood wheels and porcupine grass seed bodies (Fig. 5B). Designs included both a single bioderived seed body glued to the center of two wheels (Fig. 5B, 5Ci, 5Cii), as well as an altered modular design with two seeds acting as the body of the crawling structure (Fig. 5Cii). The wheels were attached to the seed bases using hot glue. In the modular design, the two seeds comprising the body were glued together before the wheels were attached. The crawling motion was conducted on a 150°C hot plate with a paper cover (Fig. 5D). Tracker video analysis and modeling software was used to quantify the path of locomotion. Figure 5E shows every 5 frames of 100x video, as used to quantify each point of motion.

**Performance.** The relatively large number of twists innate to the seed's tightly twisted structure allow the seed to "crawl" through a distinct, repeated motion. This results in increased actuation speed: by controlling the geometric parameters of the seed, the seed has repeated motion while under a single condition change (i.e. the robot completes multiple oscillations for each humidity cycle).

The seed's natural twisting movement thrusts the back wheel in a circumferential motion until it takes the place of the front wheel (Fig. 5A). This crawling motion occurs when stimulated by a change in environmental humidity conditions, and reaches optimal speed in a heated environment. While the conditions are held constant, the seed continues to crawl forward until the body reaches its full twisted state. Due to the diffusion-based mechanics of the rotation, the speed of locomotion decreases with the cycle of rotation (Fig. 5F). Each cycle of rotation is defined by the intercept of the displacement of wheel A and wheel B. There is an initialization time of approximately 2.22 min before the locomotion begins. The initial cycle has an average speed of 14.4 mm/min (0.361 BL/min), with a secondary speed of 10.8 mm/min (0.269 BL/min), and tertiary speed of 4.58 mm/min (0.064 BL/min) ( $n = 5$ ). The biohybrid design allows the seed to travel in repeated linear motion while facing a single environmental change.

The biohybrid crawling robot has nearly circular step-motion. The circumferential motion of the rear wheel produces an average ratio of 0.45 between the length of the body of the natural harvested twisting actuator and the distance the system travels in one rotation (Fig. 5A). The relation between the length of the seed and the distance traveled mimics that of the radius and diameter of a circle, with mean deviation of less than 4% from a perfectly circular path ( $n = 5$ ). The adapted biohybrid seed and wheel system generates geometric motion, regardless of the length of the body and diameter of the wheel. These parameters can be controlled to optimize the trajectory's path and speed.

Our biohybrid crawling design also supports a modular two-seed system. The multi-seed system (Fig. 5Cii) functions with the same locomotion trajectory as the single seed design, demonstrating the potential for further modulation of the crawling design. Due to the trajectory of the locomotion being circumferentially proportional to the body length (see Fig. 5A), modular design presents opportunities to further control the geometry and increase the overall speed of locomotion.

Considering the bioderived natural material of the twisted actuator, the results show a high level of consistency. The organic material has natural variation in the length of the body and the number of twists it contains. However, with controlled harvesting of the seed's body combined with the addition of biodegradable wood wheels, circular step-motion and overall linear motion is easily controlled and attainable.

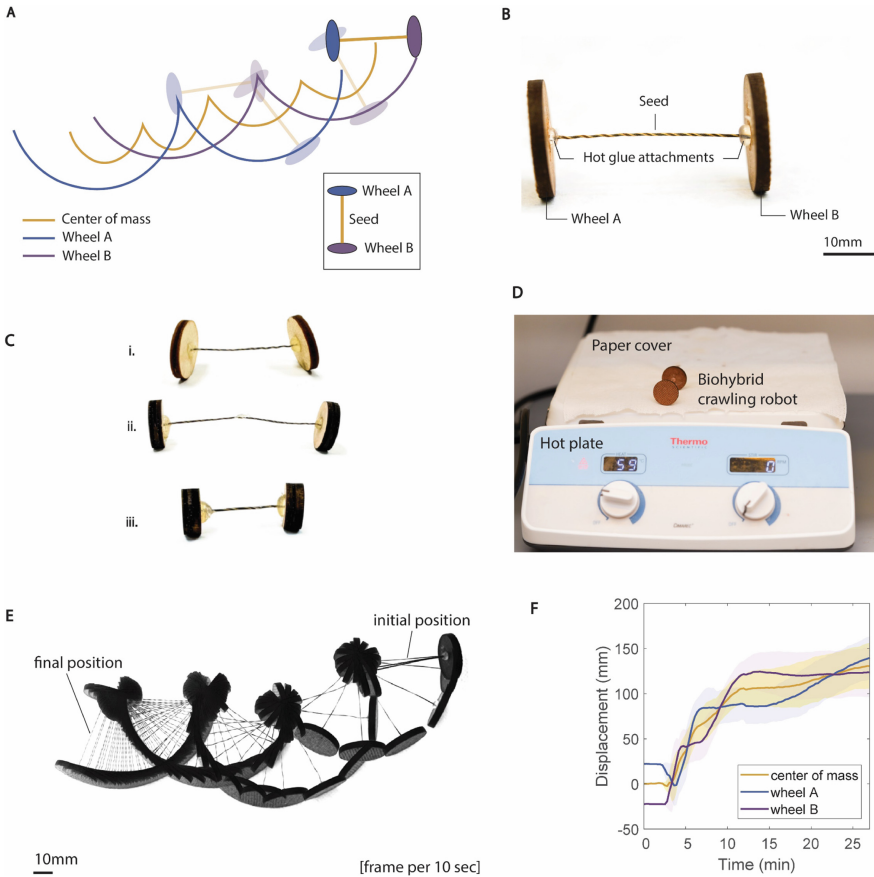


**Fig. 5.** Biohybrid crawling design. (A) Circumferential motion of the crawling system, with wheels A and B alternating motion, and the center of mass traveling approximately half of the distance of each wheel’s path. (B) Image of biohybrid crawling design with dehydrated seed as the body. (C) Three biohybrid crawling systems with differing seed lengths and wheel sizes. (D) Experimental setup of the biohybrid crawling system. (E) Time lapse of the biohybrid crawling system and the alternating motion of wheels A and B, with frames at 10 s intervals of motion. (F) The distance each wheel and the center of mass travel with respect to time. The data are means and the standard deviation is shown in the shaded regions, given  $n = 5$  samples.

### 4 Conclusion

Through harvesting the twisted body of the porcupine grass seeds, *Hesperostipa Spartea*, we produce a bioderived hygromorphic twisted actuator that converts atmospheric water concentration into mechanical energy. Biohybrid design further creates the potential for translating the seed’s natural self-burial motion into untethered, self-powered soft robotic applications. With rotational velocity dependent on environmental relative humidity and temperature, a maximum rotation of  $90^\circ/\text{sec}$  can be achieved in submergence of  $100^\circ\text{C}$  water. The seed is able to function as a twisted actuator, producing rotational motion

and load lifting, under large relative loads over 11,000 times its body mass. The unique twisted body of the seed allows for natural locking, and when this is harnessed, the interlocked seed system can withstand a mass 3,600 times its own. By utilizing biohybrid design to further leverage the twisting actuation of the seed, a crawling system can be constructed, with a forward locomotion rate of 14.4 mm/min. The guiding principles of sustainability demand that the future of robotics must be biodegradable after their life span, and our bioderived hygromorphic twisted actuator has the ability to meet these demands. We expect that through future research, our bioderived actuator will be embedded into more complex robotic systems, providing a sustainable solution to the field of soft robotics.

**Acknowledgements.** This work was supported by National Science Foundation Grants Career IIS-2047912 and IIS-2017008.

## References

1. Holstov, A., Bridgens, B., Farmer, G.: Hygromorphic materials for sustainable responsive architecture. *Constr. Build. Mater.* **98**, 570–582 (2015)
2. Reyssat, E., Mahadevan, L.: Hygromorphs: from pine cones to biomimetic bilayers. *J. R. Soc. Interface* **6**(39), 951–957 (2009)
3. Kay, R., Nitiema, K., Correa, D.: The bio-inspired design of a self-propelling robot driven by changes in humidity, Berlin, Germany, pp. 233–242 (2020)
4. Krapež Tomec, D., Straže, A., Haider, A., Kariž, M.: Hygromorphic response dynamics of 3D-printed wood-PLA composite bilayer actuators. *Polymers* **13**(19), 3209 (2021)
5. Le Duigou, A., Castro, M., Bevan, R., Martin, N.: 3D printing of wood fibre biocomposites: from mechanical to actuation functionality. *Mater. Des.* **96**, 106–114 (2016)
6. Poppinga, S., Schenck, P., Speck, O., Speck, T., Bruchmann, B., Masselter, T.: Self-actuated paper and wood models: low-cost handcrafted biomimetic compliant systems for research and teaching. *Biomimetics* **6**(3), 42 (2021)
7. Reichert, S., Menges, A., Correa, D.: Meteorosensitive architecture: biomimetic building skins based on materially embedded and hygroscopically enabled responsiveness. *Comput. Aided Des.* **60**, 50–69 (2015)
8. Menges, A., Reichert, S.: Material capacity: embedded responsiveness. *Archit. Design* **82**(2), 52–59 (2012)
9. Wood, D.M., Correa, D., Krieg, O.D., Menges, A.: Material computation—4D timber construction: towards building-scale hygroscopic actuated, self-constructing timber surfaces. *Int. J. Archit. Comput.* **14**(1), 49–62 (2016)
10. Rüggeberg, M., Burgert, I.: Bio-inspired wooden actuators for large scale applications. *PLoS ONE* **10**(4), e0120718 (2015)
11. Tahouni, Y., et al.: Programming sequential motion steps in 4D-printed hygromorphs by architected mesostructure and differential hygro-responsiveness. *Bioinspir. Biomim.* **16**(5), 055002 (2021)
12. Le Duigou, A., Correa, D.: 4D printing of natural fiber composite. In: *Smart Materials in Additive Manufacturing, Volume 1 : 4D Printing Principles and Fabrication*, pp. 297–333. Elsevier (2022)
13. Fu, L., et al.: A humidity-powered soft robot with fast rolling locomotion. *Research*, **2022**, 2022/9832901 (2022)

14. Shin, B., et al.: Hygrobot: a self-locomotive ratcheted actuator powered by environmental humidity. *Sci. Robot.* **3**(14), eaar2629 (2018)
15. Burgert, I., Fratzl, P.: Actuation systems in plants as prototypes for bioinspired devices. *Phil. Trans. R. Soc. A.* **367**(1893), 1541–1557 (2009)
16. Kim, B.H., et al.: Three-dimensional electronic microfliers inspired by wind-dispersed seeds. *Nature* **597**(7877), 503–510 (2021)
17. Luo, D., et al.: Autonomous self-burying seed carriers for aerial seeding. *Nature* **614**(7948), 463–470 (2023)
18. Fiorello, I., Margheri, L., Filippeschi, C., and Mazzolai, B.: 3D micromolding of seed-like probes for self-burying soft robots. 2022 IEEE 5th International Conference on Soft Robotics (RoboSoft), pp. 255–260. IEEE, Edinburgh (2022)
19. Cecchini, L., Mariani, S., Ronzan, M., Mondini, A., Pugno, N.M., Mazzolai, B.: 4D printing of humidity-driven seed inspired soft robots. *Adv. Sci.* **10**(9), 2205146 (2023)
20. Geer, R., Iannucci, S., Li, S.: Pneumatic coiling actuator inspired by the Awns of *Erodium Cicutarium*. *Front. Robot. AI* **7**, 17 (2020)
21. Molano-Flores, B.: Diaspore morphometrics and self-burial in *Hesperostipa Spartea* from loam and sandy soils. *J. Torrey Bot. Soc.* **139**(1), 56–62 (2012)
22. Jung, W., Kim, W., Kim, H.-Y.: Self-burial mechanics of hygroscopically responsive Awns. *Integr. Comp. Biol.* **54**(6), 1034–1042 (2014)
23. Yanez, A., Desta, I., Commins, P., Magzoub, M., Naumov, P.: Morphokinematics of the hygroactuation of feather grass Awns. *Adv. Biosys.* **2**(7), 1800007 (2018)